# Reduction in mechanical anisotropy through high temperature heat treatment of Hastelloy X processed by Selective Laser Melting (SLM)

**T Etter[1], K Kunze[2], F Geiger[1] and H Meidani[1]**
[1] ALSTOM (Switzerland) Ltd, Baden, Switzerland
[2] Scientific Centre for Optical and Electron Microscopy, ETH Zurich, Switzerland
E-mail: thomas.etter@power.alstom.com; karsten.kunze@scopem.ethz.ch; fabian.geiger@power.alstom.com; hossein.meidani@power.alstom.com

**Abstract.** Selective Laser Melting (SLM) is an additive manufacturing technology used to directly produce metallic parts from thin powder layers. To evaluate the anisotropic mechanical properties, tensile test specimens of the Ni-base alloy Hastelloy X were built with the loading direction oriented either parallel (z-specimens) or perpendicular to the build-up direction (xy-specimens). Specimens were investigated in the "as-built" condition and after high temperature heat treatment. Tensile tests at room temperature and at 850°C of "as-built" material have shown different mechanical properties for z- and xy-specimens. The anisotropy is reflected in the Young's modulus, with lower values measured parallel to the build-up direction. It is shown that the anisotropy is significantly reduced by a subsequent recrystallization heat treatment. The characterization of microstructural and textural anisotropy was done by Electron Back Scatter Diffraction (EBSD) analysis. Predictions of Young's modulus calculated from the measured textures compare well with the data from tensile tests.

## 1. Introduction

Ni-base superalloys are extensively used for components in aero- and industrial gas turbine engines [1, 2]. The solid-solution strengthened Ni-base alloy Hastelloy X has been widely used in today's heavy-duty gas turbines for hot gas path components such as combustors, transition pieces and exhaust-end components [3]. Progress in Ni-base alloy performance would not be possible without the parallel improvement of processing technology. Additive manufacturing processes such as selective laser melting (SLM) [4, 5] are prospective candidates to complement or replace conventional machining/production processes such as cutting and casting. Due to powder based article production and the inherently high cooling rates in these processes, the resulting material is very homogeneous with respect to chemical composition and principally free of segregations and residual eutectic phases [6, 7].

The high thermal gradients in SLM processing cause crystals to grow preferentially in well-defined directions, resulting in specific microstructures and textures [8]. Suitable scanning strategies favor either sharp single component textures or more uniformly distributed crystal orientations [9]. The anisotropy of mechanical properties is largely controlled by the texture and can be modeled based on the texture and the single crystal mechanical properties [10, 11]. In the present study, texture and microstructural anisotropy in SLM made Hastelloy X specimens are analyzed using EBSD (electron backscatter diffraction) and correlated with anisotropic material behavior observed during mechanical testing (Young's modulus). We report on processing routes to reduce the amount of anisotropy by (i) optimized laser scanning strategy, and (ii) suitable heat treatment.

## 2. Material and methods

### *2.1. Sample processing and testing*

In the SLM process, thin powder layers are deposited on a metallic base plate or on the already produced skeleton of a designed object [12]. The cross-sections of a sliced CAD file are scanned subsequently using a high power laser beam in order to locally melt the powder material. The Hastelloy X alloy powder (www.praxairsurfacetechnologies.com) has a nominal weight percentage composition of 22% Cr, 18% Fe, 9% Mo, 1.5% Co, 0.7% W, <1% Si, <1% Mn, 0.10% C, <0.008% B, Ni (balance). A SLM machine 280HL (www.stage.slm-solutions.com) was used to build specimens with different orientations relative to build-up (z-axis) and laser scanning directions (in the xy-plane).

Three different laser scanning strategies were performed for subsequent layers with nominal

thickness of 30 µm deposited in the xy-plane (one fixed scanning direction per layer; see also Fig. 1, top):

A. lines rotate 90° (parallel/perpendicular to the testing direction),
B. lines rotate 90° (+45°/-45° to the testing direction),
C. lines rotate 67°.

The SLM built pieces were cut from the substrate plate by electro-discharge machining. Samples were investigated either in the "as-built" condition or after heat treatment at 1200°C for 4h (Table 1). Tensile tests of M10 specimens were carried out according to ISO 6892 at ambient and elevated temperature (850°C) with a 50 kN load cell, at a strain rate of ~4 %/min, with a hold time of ~30 min after reaching the testing temperature in a resistance furnace.

*2.2. Characterization*

Metallographic sections were cut from the thread areas of the tensile test specimens for microstructural characterization. Orientation mappings were performed on a FEG-SEM MIRA3 XMU (www.tescan.com) equipped with an AZtec EBSD system (www.oxford-instruments.com), or on a FEG-SEM Quanta 200F (www.fei.com) equipped with a Hikari EBSD module and software OIM 6.2 (www.edax.com) enabling large area combo scans. EBSD data acquisition was carried out at 20 kV acceleration voltage, 15-25 mm working distance, and a nominal beam current of 2-7 nA. Only reliable data (confidence index > 0.1) were used for texture representation and subsequent modeling.

*2.3. Texture based property modelling*

The elastic tensor for single crystal Hastelloy X ($c_{11}$ = 230.40 GPa, $c_{12}$ = 156.12 GPa, $c_{44}$ = 121.77 GPa at room temperature, derived from [13]) possesses a marked anisotropy, with minimum of Young's modulus of 104 GPa parallel to <100> and maximum of 294 GPa parallel to <111>. Using the MATLAB toolbox Mtex [14] (http://code.google.com/p/mtex/), we derived texture based lower (Reuss) and upper (Voigt) bounds of the polycrystal elastic property, as well as their arithmetic average (Hill estimate) [15].

Table 1: Young's modulus measured on SLM specimens processed by three scanning strategies.

| **Specimen testing direction** | **Heat treatment** | **Test Temperature [°C]** | **Scanning strategy** | | |
|---|---|---|---|---|---|
| | | | A (0°/90°) | B (-45°/45°) | C (random) |
| | | | **Young's Modulus [GPa]** | | |
| XY | as-built | 23 | 146 | 190 | 171 |
| XY | as-built | 850 | 99 | 129 | 118 |
| XY | 1200°C/4h | 23 | 195 | 198 | 192 |
| XY | 1200°C/4h | 850 | 136 | 132 | 139 |
| Z | as-built | 23 | 148 | - | 148 |
| Z | as-built | 850 | 101 | - | 106 |
| Z | 1200°C/4h | 23 | 182 | - | 187 |
| Z | 1200°C/4h | 850 | 121 | - | 130 |

## 3. Results

*3.1. Mechanical testing*

The experimental results (Table 1) indicate a major impact of the scanning strategy on the mechanical anisotropy measured in the as-built condition at room and elevated temperature. Young's modulus hardly differs for z-specimens (parallel to the build-up direction) between strategies A and C, which also matches the value in the xy-plane for strategy A (i.e. parallel to the laser scanning direction). After heat treatment, the differences between the three scanning strategies are nearly extinct, and the anisotropy of the modulus is largely reduced [16].

*3.2. Microstructure and texture analysis*

Metallographic observations as well as orientation mapping (by EBSD) on as-built specimens reveal a columnar grain morphology, with the longer grain axes aligned preferentially parallel to the build-up direction z. A grain boundary pattern roughly parallel to the two perpendicular

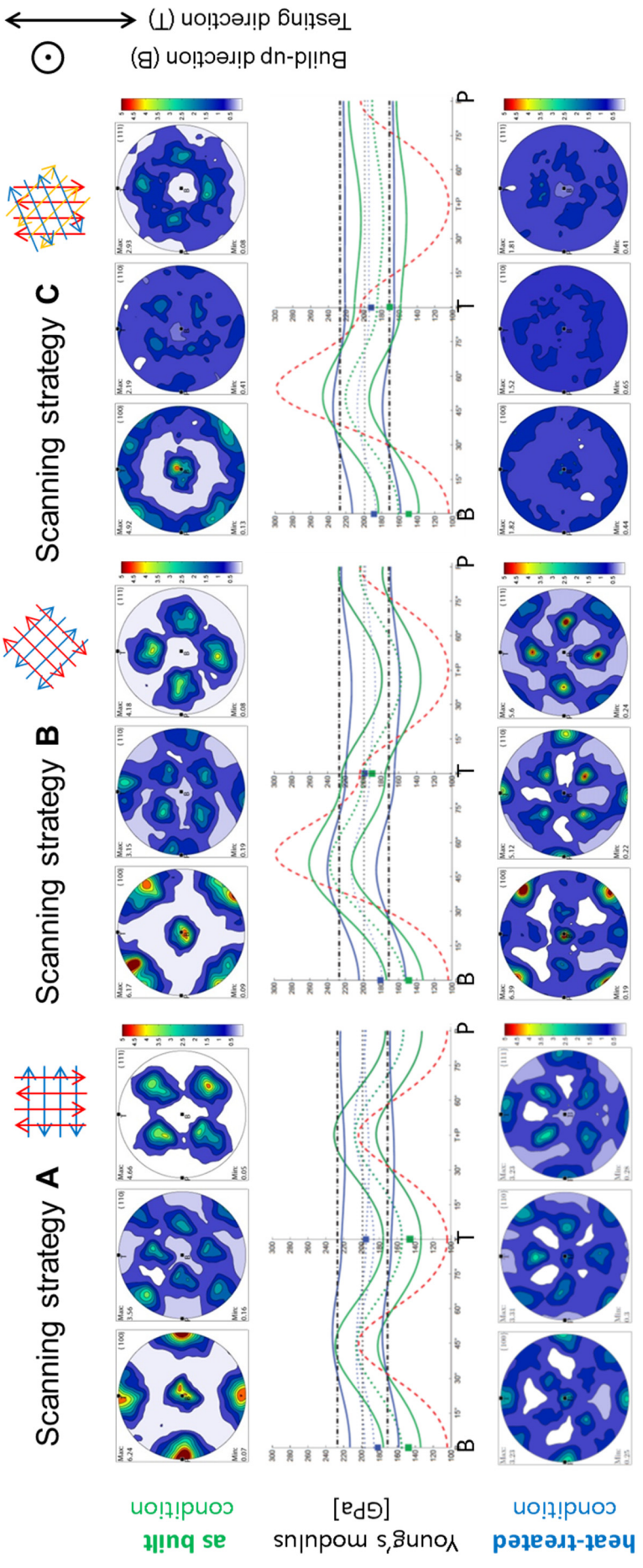


**Fig. 1**
Texture (pole figures) and derived Young's modulus (profiles B-T-P) for Hastelloy X specimens, processed by SLM with scanning strategies A, B and C. The profiles show Young's modulus for a single crystal (red dashed), for the textured material in as-built (green) and in heat-treated (blue) condition, and for the isotropic case of a uniform texture (black dash-dot). Upper (Voigt) and lower (Reuss) bounds by solid lines, Hill average by dashed lines.

laser scanning directions was observed in the xy-plane of samples processed by strategies A and B. All samples possess a pronounced texture with a concentration of <001> parallel to the build-up direction z (Fig. 1, top row). For A and B strategies, the <100> axes align preferentially parallel to the respective laser scanning directions, thus the textures are basically single components <100>{001} for A and <110>{001} for B with some scatter, when referred to testing and build-up direction. For scanning strategy C, a rather random distribution of <100> within the xy-plane was observed, thus a fiber texture with <001> parallel to z.
After heat treatment, the microstructure is largely modified by recrystallization, resulting in significant grain coarsening and more equiaxed grain shapes. No indications of the as-built columnar grain shapes are remaining. On the other hand, a larger part of the materials has retained the as-built texture, which is complemented by additional texture components and a higher uniform component (Fig. 1, bottom row), resulting generally in a reduction in texture strength from as-built to heat-treated conditions.

### *3.3. Texture based property modelling*

Young's modulus is predicted from the texture for any desired sample direction and plotted as profile from B (build-up direction z) to T (testing direction) and further to P (perpendicular to both) (Fig. 1, center row). For comparison, the corresponding profiles are also shown for an ideally oriented single crystal (red dashed lines). The anisotropy for the single crystal is maintained in type, but reduced in extent for the textured samples in as-built condition for scanning strategies A and B, while there is only little in-plane (xy) anisotropy for strategy C. The broadening of textures after heat treatment result in further reduced anisotropy of Young's modulus, which approaches the isotropic bounds in the xy-plane for strategy C. For all three strategies, Young's modulus still maintains a minimum parallel to the build-up direction z, caused by a maximum in the center of the (001) pole figure.

## 4. Discussion and conclusions

It was shown that suitable scanning strategies allow tailoring the texture and thus anisotropy of mechanical properties. Rotation of the laser scanning direction by 90° between consecutive layers results in single texture components and minima of Young's modulus along the build-up and laser scanning directions. Rotation of the laser scanning direction by 67° leads to <001> fiber textures and to a nearly transverse isotropic elastic tensor, both with respect to the build-up direction. Additional texture components develop by recrystallization through suitable heat treatment, which generally reduce the overall elastic anisotropy. The SLM technology enables to control the crystallographic textures with respect to two distinct sample directions (build-up and laser scanning), which offers new possibilities optimizing the design of components, either for minimized anisotropy or taking advantage of a suitably maximized anisotropy.

## References

1. Durand-Charre M and Davidson JH 1997 *The microstructure of superalloys* (Amsterdam: Gordon and Breach Science Publ.) 124 S.
2. Sims CT 1987 *Superalloys II [high-temperature materials for aerospace and industrial power]* (New York, N.Y.: Wiley) 615 S.
3. Zhao JC et al 2000 Mat Sci Eng A **293** 112-119.
4. Das S et al 2000 Mater Design **21**(2) 63-73.
5. Marquis FDS et al 2002 *Rapid prototyping of materials proceedings of symposium* (Warrendale, Pa.: TMS) 224 S.
6. Rickenbacher L et al 2013 Rapid Prototyping J **19**(4) 282-290.
7. Wang F 2012 Int J Adv Manuf Technol **58**(5-8) 545-551.
8. Kunze K et al 2014 Mat Sci Eng A **620** 213-222.
9. Thijs L et al 2013 Acta Mater **61**(5) 1809-1819.
10. Kocks UF et al 1998 *Texture and anisotropy preferred orientations in polycrystals and their effect on materials properties* (Cambridge: Cambridge University Press) XII, 676 S.
11. Niehuesbernd J et al 2013 Mat Sci Eng a-Struct **560** 273-277.
12. Rombouts M et al 2006 Cirp Ann-Manuf Techn **55**(1) 187-192.
13. Canistraro HA et al 1998 J Eng Mater-T Asme **120**(3) 242-247.
14. Bachmann F et al 2010 Solid State Phenomena **160** 63-68.
15. Mainprice D et al 2011 in *Deformation Mechanisms, Rheology and Tectonics: Microstructures, Mechanics and Anisotropy* ed Prior DJ et al (Geological Society: London). 175-192.
16. Etter T et al 2014 TMS2014 143rd annual meeting & exhibition, 230.